MACHINE INTELLIGENCE RESEARCH

ISSN:2731-538X | E-ISSN:2731-5398

Vol. 17 No. 02 (2023)

DISPLACEMENT OF THE KSHETRAPAL LANDSLIDES CHAMOLI IN THE HIMALAYAN REGION USING UAV AND TLS

Ashok Anand[1]* and Alok Bhardwaj[2]

Department of Civil Engineering,
Indian Institute of Technology Roorkee - 247667, Uttarakhand, India
Email ID: a_anand@ce.iitr.ac.in

ABSTRACT

Landslides are a significant source of concern in the Himalayan region and other hilly regions of India, particularly during the wet seasons. At the same time, this is the case in the Chamoli region, which is the focus of this research. Although this is the case, there is still a deficiency in the amount of comprehensive study and a sufficient database on landslides in these regions. With respect to landslip inventory, susceptibility mapping, and risk assessment, the purpose of this study is to present a comprehensive review of the existing advances, gaps, and future directions in the Indian context. When there is a lack of data, the major objective is to make use of geospatial platforms in order to construct a landslip inventory map that covers a number of different time periods. An evaluation of the landslip susceptibility map will be carried out with the use of the weights of evidence (UA). A total of 293 landslip polygons were manually digitised during the first stage, which took place between 2011 and 2013. With the assistance of Google Earth® and the Indian earth observation visualisation technology known as BHUVAN, this was made within the realm of possibility. On the other hand, fourteen factors that were shown to be responsible for landslides were chosen based on the findings of the earlier analysis. For example, There are a variety of components that fall under this category, including geology, geomorphology, soil type and depth, slope angle and aspect, relative relief, distance to lineaments, streams, roads, land use/cover, altitude zones, faults and thrusts, and more. As part of the process of developing a map of landslip susceptibility, both the UAV and the TLS technique were used.. This was accomplished by giving weights to each category of characteristics that were responsible for the landslip. The final landslip susceptibility map was then broken down into five distinct categories: very low, very high, medium, and low. the highest category was extremely low. After that, the IDRISI SELVA 17.0 programme was used in order to carry out a validation check on the landslip susceptibility map. This includes comparing the map to a selection of landslides that were chosen at random.

Key Words-: Displacement, Himalayan Region, Landslides, UAV And TLS.

INTRODUCTION

"Reactivation of ancient landslides" is a phrase that is used to describe the process of remobilizing landslide deposits that have been created by natural catastrophes, human

ISSN:2731-538X | E-ISSN:2731-5398

Vol. 17 No. 02 (2023)

meddling, or other factors that induce landslides, such as earthquakes or extended periods of rainfall. In contrast to rock avalanches and collapses, reactivated landslides often undergo deformation at a more gradual speed and continue for a longer period of time. For the purpose of early landslip hazard identification and emergency management, it is essential to have a comprehensive knowledge of the factors that cause reactivated ancient landslides, as well as the mechanisms that cause them to originate and the movement dynamics that they use. As part of their risk management plan, hilly areas that have big populations and are susceptible to landslides are required to have a system in place that can monitor their development.

Total stations, the Global Navigation Satellite System (GNSS), and crack monitoring devices are examples of the single-point technologies that are used in the traditional ways of landslip monitoring. Through the documentation of the relative or absolute displacement of monitoring locations, these sensors or pieces of equipment provide an accurate depiction of the progression of the landslip. Even though these conventional methods of monitoring are quite accurate, the monitoring range that they provide is restricted due to the dispersion of the monitoring equipment and the number of monitoring devices. This indicates that they are not very excellent at reflecting the overall deformation features of large-scale landslides; nonetheless, they are quite effective when it comes to monitoring the deformation of landslides at a local level [11]. As a result of recent developments in remote sensing technology, it is now feasible to gather topographical data on a large scale. This makes it much simpler to identify and monitor landslides. An example of a platform-based remote sensing technology is the use of spaceborne high-resolution satellites and Synthetic Aperture Radar (SAR). Another example is the use of airborne light detection and ranging (LiDAR) and photogrammetry using unmanned aerial vehicles (UAV) are two related technologies.. Finally, a third type of device is ground-based, which includes Ground-Based Interferometric SAR (GB-SAR) and Terrestrial Laser Scanning (TLS). For example, studies on the sensitivity of landslides, monitoring of deformation, and the detection of large-scale landslide threats have all been proved to be productive applications of spaceborne technology. The precision and depth of field that can be achieved from aerial or ground-based equipment, on the other hand, are not something that these devices can compete with. Because of this, GB-SAR is able to identify slope deformation of a few millimetres in a short amount of time and with high accuracy, while TLS may need several millimetres to assemble its point clouds. As a result of their adaptability and versatility, airborne remote sensing technologies are very useful for a variety of tasks, including the collection of data, the monitoring of deformation, and the mapping of landslip susceptibility. In contrast, airborne remote sensing technologies offer monitoring ranges and accuracy levels that are somewhere in the midst of what spaceborne and ground-based sensors give. This is because airborne sensors are able to fly through the air.

Although both TLS and GB-SAR are extremely accurate, the effective monitoring range of both approaches in surface deformation investigations may be restricted owing to topographic limits.

ISSN:2731-538X | E-ISSN:2731-5398

Vol. 17 No. 02 (2023)

This is the case even if both methods are quite exact. In situations when there are visible impediments, it may be difficult to collect precise topographical information. This is the outcome that occurs as a consequence of the fact that the scanner site can only be put in locations where people can physically access it. On the other hand, landslip monitoring that makes use of airborne unmanned aerial vehicle (UAV) technology offers a more expansive observation angle and accomplishes precise data synchronisation primarily via the deployment of a large number of ground control points (GCPs). Due to the fact that these GCPs are often organised in accordance with portable real-time kinematics (RTK) or global positioning systems (GPS), the quantity and dispersion of GCPs are the crucial factors that determine the quality of the data that is obtained by unmanned aerial vehicles (UAVs). It is often difficult to deploy sufficient human ground control points (GCPs) in the research region due to the presence of mountains, valleys, and potentially hazardous disaster zones. It is probable that surface difference analysis employing multi-phase terrain data may become difficult as a result of this, and the accuracy of data obtained by unmanned aerial vehicles (UAVs) about the terrain may decrease. The use of post-processing kinematics (PPK), which is an additional tool to manual ground control points (GCPs), is intended to further enhance the accuracy of the data gathered by unmanned aerial vehicles (UAVs). It is still possible to apply this strategy in situations when manual GCPs are not accessible. However, it is not particularly strong at handling deformation analysis, and it is often only useful for obtaining topographic data with a low resolution or surface elevations.

LITERATURE REVIEW

Larson, K. P., Godin, L., & Price, R. A. (2010). One is able to distinguish the higher and lower portions of the Greater Himalayan series of rocks when they are located inside. The two sections showed deformation with about comparable proportions of components that were coaxial and those that were noncoaxial. The temperature range that contributed to the occurrence of this deformation was between 450 and 640 degrees Celsius. In the top Greater Himalayan range, the peak temperature at which metamorphism occurs is virtually always the same. On the other hand, comparable estimates of metamorphic pressure indicate a downward trend of around 620 bars per km throughout the same region. Increasing structural depth, on the other hand, results in a drop in both the metamorphic pressure and temperature in the lower Greater Himalayan series. It is believed that the inverted gradient in the bottom half was generated as a result of the downward extension and coeval exhumation, in conjunction with the progressive addition of new rock to the Greater Himalayan series. The upper Greater Himalayan series features an abnormal pressure gradient as a result of the approximately fifty percent vertical thinning that takes place during southerly displacement. One of the most distinguishing characteristics of the deformation that occurred in the top portion of the Greater Himalayan range was flow extension, often known as flow. On the other hand, the predominant kind of deformation at the base of the series was compressing flow, which may also be described as compression perpendicular to the flow direction. In orogenic foreland zones, displacement and distortion are most often

ISSN:2731-538X | E-ISSN:2731-5398

Vol. 17 No. 02 (2023)

characterised by a flow pattern known as compressing flow. On the other hand, in deep orogenic hinterlands, same phenomena are more commonly characterised by an extended flow pattern. A key transition may be seen at the upper-lower border of the Greater Himalayan series. This transition is characterised by deformation in the hinterland style, which includes processes such as lateral midcrustal flow, and deformation in the foreland style, which includes.

Tobgay, T., McQuarrie, N., Long, S., Kohn, M. J., & Corrie, S. L. (2012). At several spots in western Bhutan, the Main Central Thrust (MCT) may be seen to bend quite a little. Along the roughly 70 km strike distance, this fold exposes the fault surface in many spots. A once-in-alifetime opportunity to track the MCT and document the magnitude and duration of the displacement has arisen due to this unusual map arrangement. There has never been an opportunity like this before. Evidence from the in situ Th-Pb geochronology of metamorphic monazite found near the MCT's hanging wall demonstrated that the prograde monazite production in rocks of the Greater Himalayan (GH) region persisted until around 20.8 ± 1.1 million years ago. In fact, cooling that happened around 15 to 10 million years ago caused in situ melts with high Y monazite overgrowths to crystallise. Lesser Himalaya (LH) prograde monazite formation in the footwall rocks necessitates that the LH footwall strata be buried at some point and that the MCT be exposed to its southernmost extent at least 15 million years ago. The era of MCT displacement is estimated to be between 20.8 ± 1.1 and 15.0 ± 2.4 million years based on the combined ages of prograde monazite in the adjoining hanging wall and footwall. The results of the dig provided the basis for this data. According to published research, shearing along the outer-
South Tibetan detachment (STD) was thought to have happened between fifteen million and twenty million years ago. This points to a period prior to that when displacement took place. The age range we provide for MCT displacement in our study agrees with our assessment, we discovered. Right adjacent to this estimate, to the north, is where our research is situated. However, the GH rocks did not start to cool until around 10 million years ago, which is five million years after the northern motion on the outer border, according to the existence of retrograde monazite grains. Both the construction of a duplex that folded the MCT without the owner's awareness and the continuation of displacement on the MCT are potential causes of this cooling. It is not out of the question that both of these things may happen. Our subsequent reconstruction results indicate a total displacement of around 230 kilometres. This is the total amount of displacement that occurred between 5.8 and 2.6 million years ago in the MCT and the structurally lower Paro Thrust. The above data suggests that the horizontal shortening rate may be determined by adding 3.2 to 4.0 and multiplying 1.3 cm/year. Neither geodetic data acquired across the Himalayas (about 1 cm/yr) nor petrologic and thermal models in central Nepal (about 2 cm/yr) anticipate such a rate of acceleration. Take note that the predicted rates of plate convergence for eastern Bhutan between 23 and 20 million years ago, which are 3.3 ± 0.7 centimetres per year, are comparable. The only option to achieve plate velocity rates in western Bhutan, according to our analysis, was to relocate the MCT. Also, at various areas in

ISSN:2731-538X | E-ISSN:2731-5398

Vol. 17 No. 02 (2023)

the Himalayas, the age of the MCT's displacement and the velocity of displacement varied considerably.

Cooper, F. J., Adams, B. A., Edwards, C. S., & Hodges, K. V. (2012). The South Tibetan Fault System (STFS) is an extensional fault that extends over 2,000 km above the peak of the Himalayas. It is also known as the South Tibetan Fault. Within the context of the tectonic processes that have occurred in the Himalayas, many individuals have arrived at a variety of interpretations about the importance of this structure. For some people, it seems to be a minuscule structure that does not have any obvious roots, despite the fact that it is widely believed to be securely planted to the north of Tibet, with offset estimates reaching over 200 km. There are a few evident constraints on the degree of slip that happens on this feature, which means that it is conceivable for there to be contradictory interpretations about this feature. There is one and only one exception to this rule, and that is the Everest area, where glacier erosion has revealed a cross section of the STFS. Direct sources of evidence, such as geothermobarometric data, have been used to support arguments that have been made in support of very huge displacements. A great number of interpretations are conceivable with regard to these considerations. The recently disclosed field studies and remote sensing data, on the other hand, add validity to the petrologic allegations that major displacements have taken place, at least in the eastern sector of the Himalaya. It would seem that the STFS trace is about 70 km off-center over the Yadong cross structure, which is a graben that is situated near to the western border of Bhutan and runs in the direction of northeast-southwest. Previous writers have suggested that this offset is the result of left-lateral movement along the Jomolhari fault system. This is the same fault system that divides the graben from the eastern boundary. Despite the fact that it may not be immediately obvious, the basic structure of the STFS actually creates a continuous low-angle detachment surface rather than an offset. According to the outcrop pattern of the structure, kinematic indications in faultrelated tectonites, and the absence of matchable correlative hanging wall and footwall units, separation must take place at a minimum velocity of around 65 kilometres. These displacements are in agreement with those of key contractional structures in the eastern Himalaya, such as the Main Central thrust system, and they contribute to the growing body of evidence suggesting the STFS extension had a significant role in the creation of the orogenic system.

MATERIALS AND METHODS

Study Area (The Chamoli District)

The Chamoli district, which is a geographical location that spans around 1936.54 square kilometres, is included in the study area. This particular region is included is an area of Uttarakhand that is often referred to as the Garhwal Himalaya. The Main Central Thrust (MCT), which is now crossing the region, is responsible for the location of the Chamoli district, which

ISSN:2731-538X | E-ISSN:2731-5398

Vol. 17 No. 02 (2023)

is a region that is currently experiencing a high level of seismic activity. It is possible that the Chamoli area may be affected by a considerable number of natural disasters, such as earthquakes, landslides, and flash floods. Heavy rains have the potential to cause landslides in the region that is the subject of this investigation. It rains a great deal less at lower altitudes and a great deal more at higher elevations within this territory under investigation. It is estimated that the annual rainfall in the northern section of Ukhimath is around 1,250.9 millimetres, while the rainfall in the centre position at Chandrapuri is approximately 1,220.1 millimetres, and the rainfall in the southern half of Ukhimath is approximately 1,220.1 millimetres. Rainfall in the Chamoli region averages around 1,485 millimetres per year. Between the months of June and September, the Chamoli area receives between seventy and eighty percent of the annual precipitation that falls on the region throughout the course of the year. During the summer, temperatures typically ranged from 27.75 to 32.54 degrees Celsius, which is much higher than the 8.32 to 13.15 degrees Celsius that were recorded during the three months of December and February. The top portion of the research area, which is comprised of 975 square kilometres, has been designated as a Kedarnath wildlife sanctuary (see Figure 1 for further information). An area that is 1641.64 square kilometres in size is drained by the Mandakini, which is the primary river. In this particular research region, the elevations range from 546 to 6840 metres above mean sea level (msl), and the slopes may be categorised as moderate to severe. Agriculture is the primary means of subsistence for the people who live in the surroundings, and the majority of the agricultural activity is located around the river and the road. Every year, at the same time period that is being investigated, the Kedarnath Temple, which is a prominent pilgrimage destination, is visited by millions of people. Since the pilgrimage destination is such a significant source of both food and revenue, the Chamoli region and the regions that surround it are very dependent on it. It was estimated that over 300,000 Indians visited the Kedarnath temple in the year 2001, but by the year 2012, the number of visitors had increased to around 572,454 according to the statistics provided by Uttarakhand tourism. This is the reason why infrastructure-driven growth is becoming more prevalent in order to satisfy the requirements of both inhabitants and tourists, which may result in changes to land use and cover. To be more specific, 92% of the overall population resides in rural regions. This means that almost all of the population lives in rural areas. A significant number of the communities that are located along the riverbed and the road. The overall population of the Chamoli district is 242,000, which is a relatively low amount when compared to the population of another district in the state of Uttarakhand. Before the census in 2001, the population density of India was 115 people per square kilometre; however, by 2011, that figure has dropped to 119 people per square kilometer.

Data Preparation

When it comes to the creation of data for landslide susceptibility mapping, there are two distinct groups: the first is the landslide inventory, which consists of polygon data, and the second is the variables that cause landslides.

ISSN:2731-538X | E-ISSN:2731-5398

Vol. 17 No. 02 (2023)

Landslide Inventory (Polygon Data of Landslides)

The multi-temporal landslip inventory is an important tool for gathering this information, which is essential for comprehending the relationship between different landslip events that have occurred in the past and the factors that led to them. The weights of evidence (UAV and TLS) approach was used in order to carry out this research. This method necessitates the collection of data from prior landslides due to the fact that the past is an essential component in forecasting the future. Prior study has shown that point location data of landslides may overlook the size or magnitude of the landslides, which may lead to biassed conclusions. This is done for the goal of mapping and analysing the susceptibility of landslides. Because of this, our research made use of a polygonal depiction of the landslip in order to reduce the impact of these unknowns. A wide variety of data sources were used in order to compile the multi-temporal landslip inventory date. A web-based geospatial platform known as BHUVAN (Indian earth observation visualisation) was one of the data sources. This platform is owned and operated by the Indian Space Research Organisation (ISRO). Consequently, in order to compile multiple-temporal landslip inventory data from 2011 to 2013, we made use of web-based platforms, publications from the government, and past research. In addition, we carried out a study of the ground truth. Extremely high rains, flash floods, and cloudbursts were the factors that led to the landslides that occurred in the Chamoli area. The first things that needed to be done were to locate the precise site of the landslip and to compose the official report. After that, the landslip locations were imported into Google Earth® using that programme. Following that, high-resolution images obtained from Google Earth® were used to demarcate the slides in order to successfully construct a multi-temporal inventory of landslides in ArcGIS. Since this was the case, we were able to form polygons out of the 293 landslides that were collected between 2011 and 2013. After some time had passed, the vector to raster conversion tool in ArcGIS was used in order to turn the landslip polygons into raster values. Once that was done, the pixel size was maintained throughout the process of resampling each landslip polygon using the standard UTM 44N zone format. We were able to effectively locate landslides by using the BHUVAN, as seen in Figure 2.

ISSN:2731-538X | E-ISSN:2731-5398

Vol. 17 No. 02 (2023)

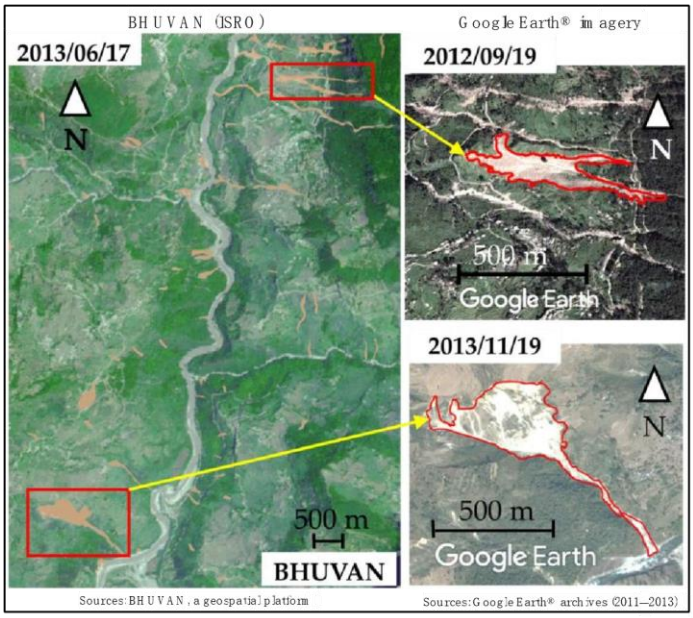

Figure 1. An example of the landslide's identification from BHUVAN (a geospatial platform)

Landslide Causative Factors

Regarding the process of susceptibility mapping, there are no strict guidelines that can be followed to determine which factors have the potential to affect landslides. In the sequence listed above, previous landslip studies, the scope of the research, the availability of data, and fieldwork in the Chamoli area were used in order to discover the variables that caused the landslip. One of the first things that we did was go through the official documentation and academic publications that were associated with the landslip vulnerability mapping for the Chamoli region. The next most significant geographical and attribute data sets that were included in this analysis were geology, geomorphology, soil type, depth, slope angle, slope aspect, relative relief, distance to thrusts, distance to lineaments, distance to streams, distance to roads, land use/cover, and altitude zones. These data sets were included in this study. Various factors that have the potential to cause landslides are explored in connection to the role that they serve in this context.

In order to build map layers that reflected lithology, geomorphology, and fundamental geological features such as thrust, fault, and lineament, the geological maps that were created by the Disaster Mitigation Management Centre (DMMC) were used. In order to construct topography-related layers with a resolution of ten metres, the stereoscopic Cartosat1 DEM provided the necessary information. This particular layer set included a number of different components, including the slope angle, slope aspect, relative relief, altitude zone, and streams

ISSN:2731-538X | E-ISSN:2731-5398

Vol. 17 No. 02 (2023)

network. A procedure of digitization was used in order to obtain road data during the BHUVAN. Using information obtained from the Landsat 8 Operational Land Imager (OLI) satellite operated by the United States Geological Survey, a map layer that represents the land use/cover map (2014) was created. Through the use of the information that we gathered from Uttarakhand, we were able to determine the kind of soil as well as the depth layers.

In this part, a concise explanation of the procedures that were carried out in order to prepare each data layer is provided. A digital elevation model (DEM) of ten metres was created using ArcGIS in order to calculate the slope angle and slope aspect angles. ArcGIS's zonal statistics tool was used in order to effect the transformation of the DEM into relative relief. For the purpose of this method, the DEM was used as zones. The hydrology tools that are available in ArcGIS were used in order to ascertain the degree of separation between the DEM and streams. The land use and cover was created with the help of ArcGIS by using a supervised classification technique that made use of the maximum likelihood methodology. It was discovered that the Landsat 8 OLI satellite had captured a picture. The Euclidean distance system was used by the spatial analyst tools of ArcGIS in order to achieve the task of measuring the distances between the many layers of streams, faults, thrusts, lineaments, and roads that are present in the terrain. The specifications that were supplied by the India Meteorological Department (IMD) were used in the process of creating the altitude zone map. The whole set of data was transformed to a raster format by making use of the identical pixels, and after that, each raster map was divided into a number of different groups. An illustration of the final results of the causal factor analysis may be seen in Figure 3.

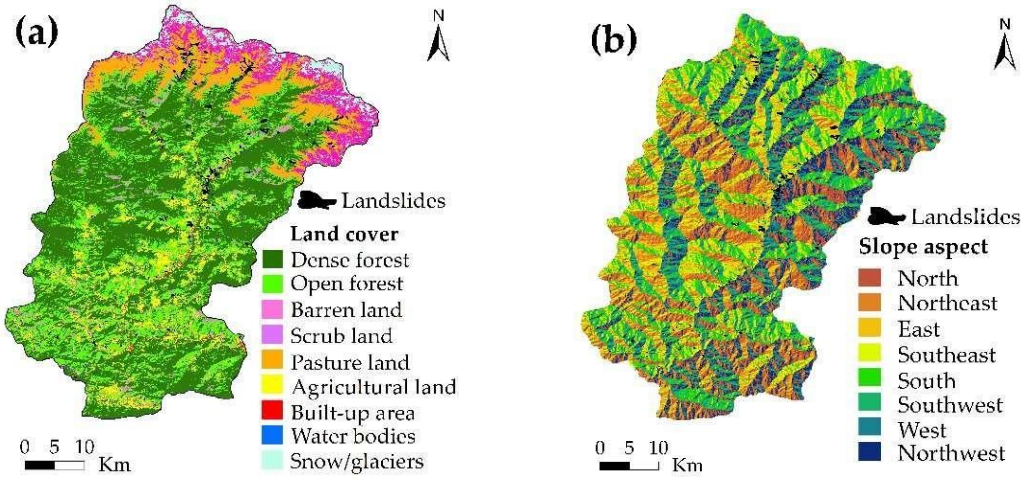

ISSN:2731-538X | E-ISSN:2731-5398

Vol. 17 No. 02 (2023)

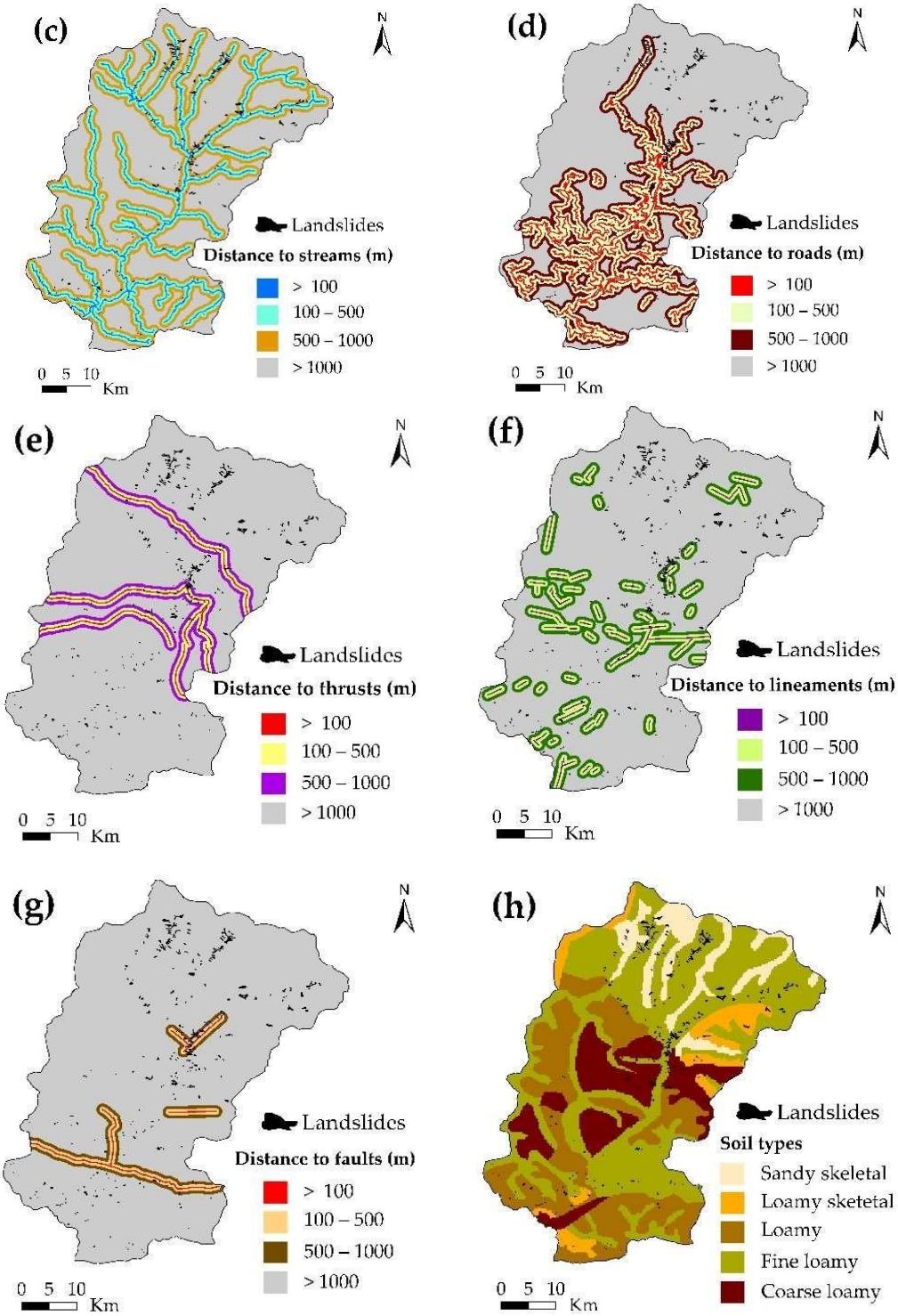

ISSN:2731-538X | E-ISSN:2731-5398

Vol. 17 No. 02 (2023)

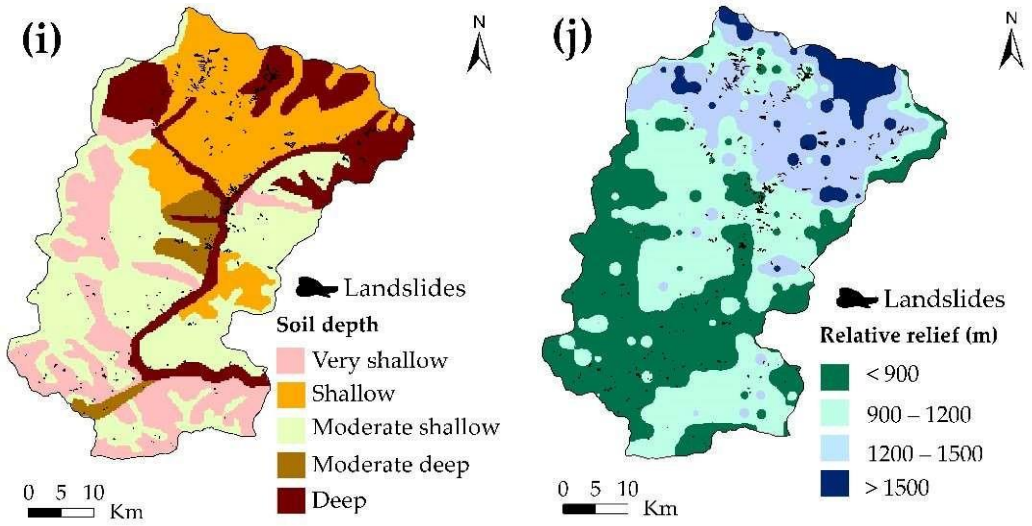

Figure 2. Landslide causative factors for the study area: (a) land-cover; (b) slope aspect; (c) distance to streams; and (d) distance to roads; (e) distance to thrust; (f) distance to lineaments; (g) distance to faults; (h) soil type; (i) slope depth; and (j) relative relief.

Methods

UAV and TLS Method

In this particular research, the weight of evidence approach was used in order to map the probability of landslides. This method integrates data from both UAVs and TLS instruments. This technique, which is driven by statistics and eliminates the subjectivity that is associated with weight, makes it simpler to identify the structural elements that were responsible for the landslip. The initial impetus for the development of UAV and TLS technology was determined to be the discovery and investigation of possible mineral resources. UAV and TLS methods have been used extensively in the process of mapping the danger of landslides in recent years. This mathematical formulation is offered by, and it also offers an in-depth explanation of the concept that is being discussed. The guiding notion that "the past is the key to the future" must be acknowledged in order for the use of the UAV and TLS plan to be successful. Therefore, it is quite probable that future landslides will take place in situations that are comparable to those that were responsible for the occurrence of prior landslides. Regarding the landslides, we are operating on the assumption that the many elements that contribute to their occurrence are conditionally unrelated to one another. It is also hypothesised that the landslides that occurred in the region that is now being investigated may have been brought on by a confluence of many causes that contributed to their occurrence. This resulted in the past landslides being taken into consideration when establishing the relative significance of the several components that are important causes of landslides by incorporating them. One strategy that takes into consideration

ISSN:2731-538X | E-ISSN:2731-5398

Vol. 17 No. 02 (2023)

all of the potential causes of landslides is the one that combines UAVs with TLS. This weight (W+ or W−) is either determined by the existence or absence of landslides within the region that has been indicated. By using this particular approach, a connection is established between the positive (W+) and negative (W−) weights that are assigned to the event, which are determined by the occurrence or non-occurrence of the event.

$$W+ = \log_e P\{B|D\} \quad (1)$$

$$W- = \log_e \quad (2)$$

This equation has the following variables: P, which stands for probability; B, which represents the presence or absence of a certain category of landslide-causing elements; D, which represents the presence of landslides; and D, which represents the complete absence of landslides. Due to the fact that the findings are presented in the form of a logarithmic table. Because of this, the difference between the two weights, which is denoted by the symbol C (C = W+ − W−), is referred to as the weight contrast. When there is a tight geographical link between the landslides and the events that caused them, the size of the contract is proportional to the proximity of the geographical relationship. The sign S(C) is used to signify the ratio that is used to determine the standardised value of C. This value is obtained by dividing C by its standard deviation. When it comes to the significance of the spatial connection between the components that influence the occurrence of a landslip, the value of the property that is referred to as Wstd is what takes into consideration. Furthermore, it provides an indication of the degree of confidence that the posterior probability has.

Do you have any idea where I might find it? "the" S2W+ and S2W− are the respective notations that are used to signify the variables that reflect positive weights (W+) and negative weights (W−), respectively. Using the formulae that are presented below, it is simple to determine the standard deviations of both positive and negative weights:

$$S2W+ = 1 + 1 \quad (3)$$

$$S2W- = \quad (5)$$

The standardised weight contrast (Wstd), which is often referred to as the ratio of the contrast to its S(C) (standard deviation), is used for the purpose of computing the confidence level.

$$Wstd = (C/S(C)) \quad (6)$$

ISSN:2731-538X | E-ISSN:2731-5398

Vol. 17 No. 02 (2023)

When a factor has a weight contrast that is positive, it is considered to be advantageous for landslides. On the other hand, when the weight contrast is negative, it indicates that the factor is not favourable for landslides. In the event that the weight contrast is somewhat near to zero, the relevance of the factor's link with the landslides is negligible. Overall, the landslip susceptibility index (LSI) is calculated by adding up the standardised weight contrasts for all of the factors that cause landslides, which are as follows: The LSI function is equivalent to the standard deviation of the component weights, which is denoted by the symbol Wstd. There is a correlation between locations with high LSI values, which are positive, and the likelihood of landslides occurring. If, on the other hand, the LSI value is low or negative, this indicates that the landslip is not very susceptible.

Validation of Landslide Susceptibility Map

Verifying the approach that is currently being used is very necessary in order to locate the most suitable model and produce an accurate map of the susceptibility of landslides. In order to ascertain whether or not the landslip susceptibility map was authentic, we calculated the relative operative characteristic (ROC) method and contrasted the proportion of landslips that were classified into each susceptibility group [133,134]. The area under the curve (AUC) of the receiver operating characteristic (ROC) is a measurement of the accuracy of a probabilistic model in predicting whether or not an event will take place. A number that is closer to 0.5 in the area under the curve (AUC) suggests that the accuracy is low, while a value that is closer to 1 shows that the accuracy is great. In order to determine the success-rate curves for this investigation, it was necessary to make use of the IDRISI SELVA17.0 software programme. Based on the findings of landslip tests and analysis of the area under the curve (AUC), it is evident that this particular model failed more often than any other.

RESULTS

Landslide Inventory Map

A total of 7.46 square kilometres, or 74,704 grid cells, are covered by landslides, which accounts for around 0.38 percent of the whole study area. For the goal of using the UAV and TLS approach, a total of 293 landslip polygons were found between the years 2011 and 2013. The finished multitemporal landslip inventory map for the district is shown in Figure 4, which can be seen here.

ISSN:2731-538X | E-ISSN:2731-5398

Vol. 17 No. 02 (2023)

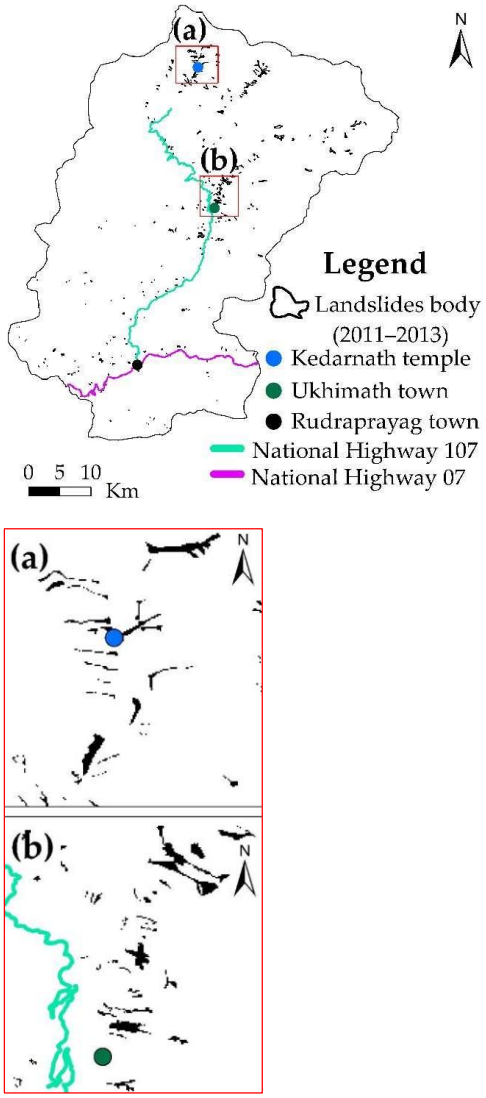

Figure 3. The distribution map of landslide body in the Chamoli district (2011–2013).

Validation of Landslide Susceptibility Map

The validity of the landslide susceptibility map was established via the process of comparing it to a random sample of landslides. The ROC (AUC) curve is shown in Figure 6, which illustrates the performance of the model. Based on the huge area under the curve (AUC) value, it seems that the strategy using UAVs and TLS was very successful. According to the created map, there are regions that are susceptible to landslides, and the forecast for such regions is correct 85.7% of the time.

ISSN:2731-538X | E-ISSN:2731-5398

Vol. 17 No. 02 (2023)

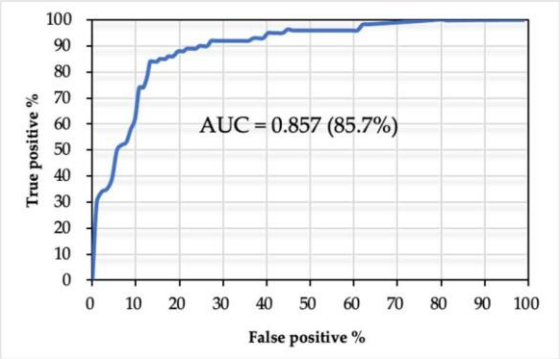

Figure 4. The graph showing validation of landslide susceptibility map under the ROC (AUC) curve using the IDRISI Selva 17.0 software.

Analysis of Landslide Susceptibility Map

The graphs of the components that have the potential to create landslides are shown in Figure 7, together with the standardised weight contract value that corresponds to each of these components. Positive and negative weight contrasts are both shown in the graphs. Both types of weight contrasts are presented. Examples of places that are devoid of forest cover include scrubland, pastureland, barren land, urban areas, and agricultural land. This lack of forest cover makes these regions more susceptible to landslides. This demonstrates, with a significant amount of data, that landscapes that are free of trees are more likely to have landslides (Figure 7a). When slope aspect was taken into consideration, classes that faced south, southeast, or west were among the most at danger (Figure 7b). when the distance to streams and highways rose, particularly when the distance reached higher altitudes, the vulnerability of the landslip decreased (by more than one thousand metres). According to the standardised weigh contract, Figure 7d demonstrates that the distance from streams and highways is highly associated to the incidence of landslides. This is the conclusion that can be drawn from the data shown earlier. It has been determined that there is a significant relationship between the incidence of landslides and geological features such as faults and Main Central Thrusts (MCTs), as shown by the standardised weight contract value. A weak relationship was found to exist near to the lineaments, as shown by the found results. In the context of this investigation, the soil types that are most susceptible to damage are fine loamy and loamy skeletal. When the soil depth was taken into consideration, the majority of landslides occurred in the shallow and deep soil classes as separate events. It was on the steep slopes of the upper watershed of the Mandakini river, where the relative relief was large (1200-1500 m), that the highest frequency of landslides occurred. It is because of this that the concept that regions with high relative relief are more likely to have landslides is given greater weight. There were high values for the slope's standardised weight contrast across all steep slopes, with the exception of those slopes that were more than 65 degrees. It rains a great deal less at lower altitudes and a great deal more at higher

ISSN:2731-538X | E-ISSN:2731-5398

Vol. 17 No. 02 (2023)

elevations within this territory under investigation. When the height of the region is higher than three thousand metres, there is a larger likelihood that a landslip may occur. It is possible that there was a deficiency of vegetation at higher elevations (more than 300 metres), which increases the probability of landslides occurring after heavy rains; this may have been a factor that led to the occurrence of this landslide. The most vulnerable lithology groups are garnetiferous gneiss, schist, and migmatite. Porphyritic gneiss and mica schist come in second and third, respectively, followed by granite gneiss, mica schist, and cale zones. Regarding the significance of the situation, these groups are very susceptible. When it comes to the geomorphology aspect, the classes that are most susceptible to damage are the glacier terrace, the alluvium terrace, and the alluvium zone. According to the findings of the research, regions that lacked trees, which are often comprised of scrubland, pastureland, and barren land, were either moderately or very susceptible to landslides. The findings also indicate that areas that are most susceptible to landslides are those that include a high altitude zone, thrusts, faults, thin soil, and steep slopes that face either the southeast, the south, or the west on the horizon.

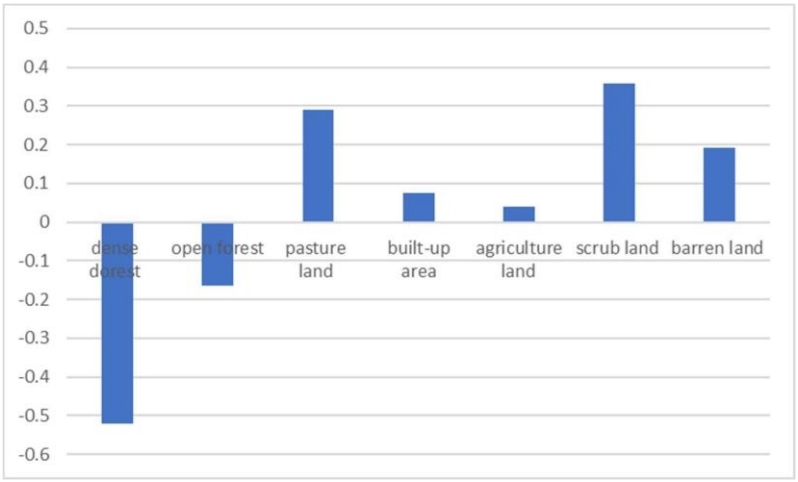

a)

ISSN:2731-538X | E-ISSN:2731-5398

Vol. 17 No. 02 (2023)

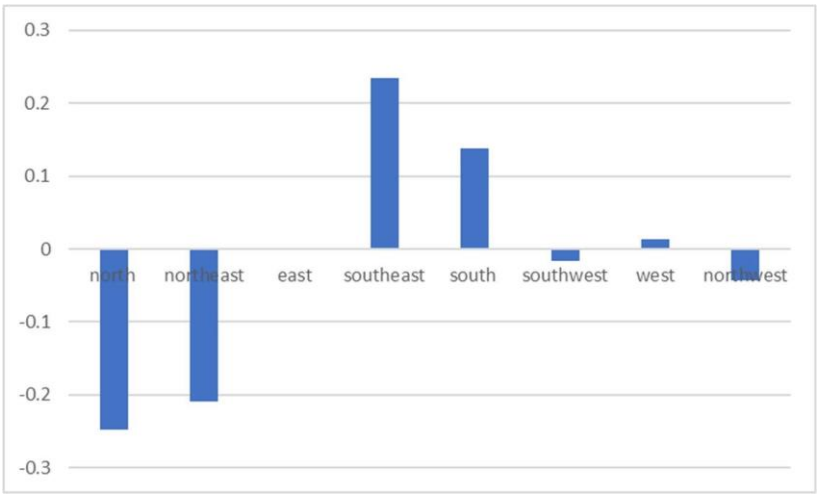

b)

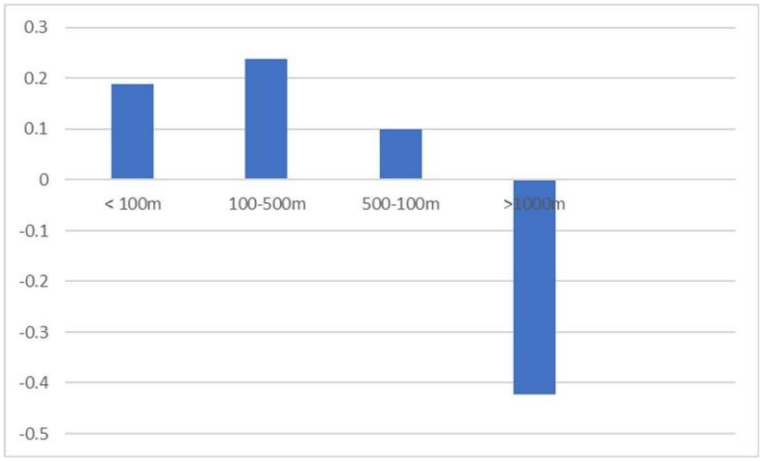

c)

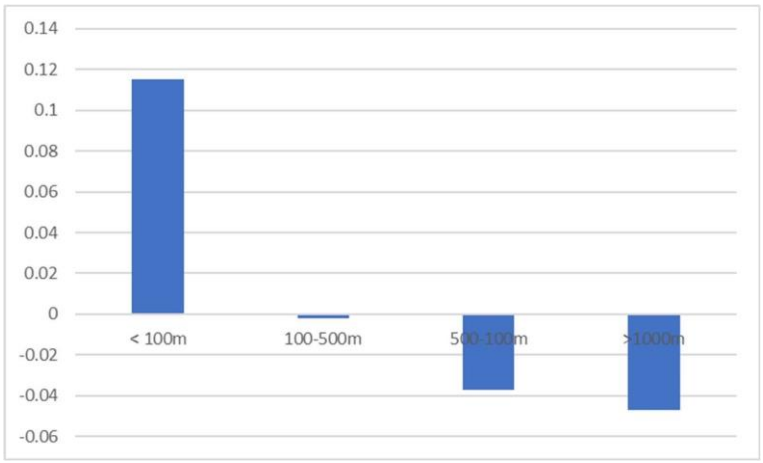

ISSN:2731-538X | E-ISSN:2731-5398

Vol. 17 No. 02 (2023)

d)

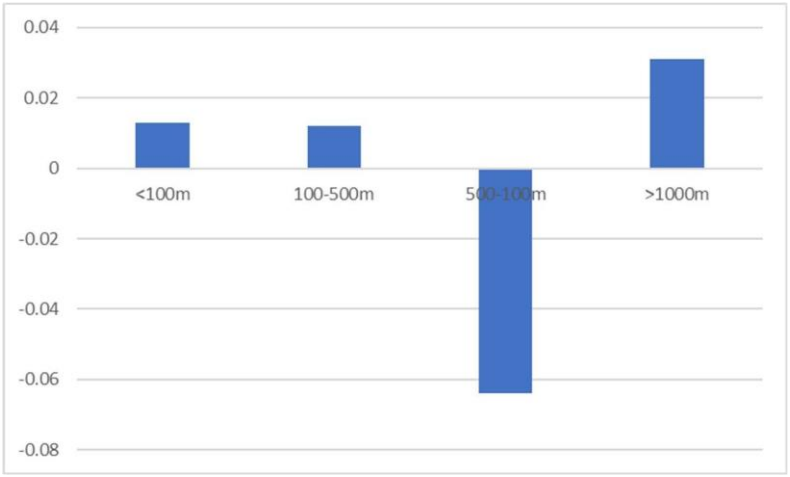

e)

Figure 5. The graphs of landslide causative factors and their corresponding standardized weight contract value: (a) land use/cover; (b) slope aspect; (c) distance to streams; (d) distance to roads; (e) distance to thrust.

DISCUSSION

Landslide Susceptibility Mapping (Present Study)

The landslip susceptibility map at the district level was developed by the use of a quantitative methodology within the framework of a Geographic Information System (GIS). The BHUVAN and web-based platforms were combined in order to create a spatio-temporal landslip inventory of the research region. This was done in order to make the most of the little data that was available. There are a number of typical hurdles that stand in the way of landslide susceptibility or hazard mapping and risk assessment in India. These include a lack of multi-temporal landslide inventory, pricey high-resolution satellite pictures, and limited landslide history records. All of these factors are the root cause of the restrictions that these techniques now possess. Additionally, owing to concerns about shadows and cloud cover, low-optical remote sensing satellite pictures would not be adequate for locating landslides in wooded regions of the Indian Himalayas. This is due to the clouds, which are to blame. The use of high-resolution satellite data is necessary for the development of improved hazard mapping and assessment skills. The conventional method of mapping landslide susceptibility depended on point data obtained during the occurrence of landslides. However, due to the fact that point data on landslide occurrences do not reflect the volume and magnitude of landslides, the amount of landslide susceptibility or hazard zonation may be distorted. Therefore, it is preferable to

ISSN:2731-538X | E-ISSN:2731-5398

Vol. 17 No. 02 (2023)

compile landslip polygon data in order to create a good map of landslip risk or susceptibility and for further evaluation connected to landslip risks.

For the purpose of this investigation, fourteen elements that led to landslides were chosen based on the availability of data and the findings of prior study conducted in the Chamoli area. The UAV and TLS approach was used in order to generate a landslip susceptibility map. This map was manufactured by giving weights to each category of the components that cause landslides. Following the passage of some time, we examined the landslide susceptibility map by contrasting it with a collection of landslides that were chosen at random in order to see how well it held up. Due to the fact that the UAV and TLS approach achieved a prediction accuracy of 85.7%, we are able to draw the conclusion that the model provided sufficient accuracy. On the other hand, previous studies have shown that the accuracy of the model may be affected by the presence of landslides as well as the collinearity of components that cause landslides. Therefore, in order to get a higher level of accuracy in the model, it is necessary to obtain the outcomes of a multicollinearity study of the phenomena's fundamental components. Clearly, the accuracy of the model is dependent on a number of different factors, some of which are as follows: the size and scope of the study area, the accuracy of the geographic and attribute data, the dependability of the landslide inventory, the degree of uncertainty in the process of digitising the data, and the identification of the primary variables that are linked to the occurrence of landslides. There was an earlier application of the UAV and TLS technology that was carried out in the Chamoli region's little watershed. This application included an evaluation of the technique's accuracy. Nevertheless, the UAV and TLS solution has not yet been put through its paces at the district level. Because of the preset ordering of geo-factors, the BIS technique is characterised by an element of uncertainty, as shown by the findings of the earlier research conducted in India. Furthermore, as is elaborated upon in further detail in, the APH technique is not without its share of uncertainties, particularly with regard to the selection and ranking of geo-factors. As a result, the UAV and TLS methodology were used in order to circumvent the subjectivity that is inherent in the BIS and APH methodologies.

The findings made it very evident that regions that lacked any kind of forest cover were from moderately to extremely susceptible to landslides. Scrubland, pastureland, and bleak landscape were three characteristics that were often seen in these places. According to the findings of our investigation, the category of land cover known as scrubland is more prone to landslides than other soil types. In earlier research as well as by the Forest Survey of India (FSI), scrubland is characterised as a forest cover that has been degraded. Because of this, it is possible that landslides in scrubland may become more frequent in the not too distant future. According to the findings of the research, metropolitan centres and agricultural territories are often located in close proximity to major roads and river systems. According to the findings of our investigation, regions that are prone to landslides that are of a medium to high severity are situated along the courses of the Mandakini River and key roadways (National roads 107 and

ISSN:2731-538X | E-ISSN:2731-5398

Vol. 17 No. 02 (2023)

07). Land that is used for agriculture and areas that are densely populated are more susceptible to landslides in these areas. According to the findings of earlier research, the study area has a total of 128 percent wooded regions and 32 percent non-forest areas. This is in addition to the fact that the majority of the areas that are not covered with forests are located on steep terrain or are otherwise elevated [14]. The findings indicate that places that have been through the process of deforestation are more prone to have landslides. As a consequence of this, regions that have steep slopes (36-45 degrees) and greater elevations (more than three thousand metres) are more likely to see landslides. What this indicates is that the upper Mandakini river basin and the steep slopes provide a significant danger of landslides.

There is a protected area that encompasses the upper catchment sections of the Mandakini River that is included within this research zone. The temples of Kedarnath and Tungnath attract a large number of visitors to these areas, which also serve as a sanctuary for those creatures that are native to the area. Increasing the relative relief may cause the size and amplitude of the landslip to rise, which can result in the whole landscape being transformed. Based on the findings of the study, the upper catchment region of the Mandakini river is known to be especially susceptible to landslides due to the relatively flat topography that it has. A consequence of this is that the hazards of landslides are an evident worry for both human activities and the operations of wildlife sanctuary facilities. An increase in soil moisture and a loss in vegetation may hasten the formation of landslides and the deterioration of shallow landslides that are caused by rainfall. This may be more likely to occur if the vegetation is reduced. It was determined that the lack of vegetation was the primary cause of the majority of the landslip incidents that occurred during this examination. The sandy skeleton and fine loamy zones were the locations where these events took place. The upper watershed and the Mandakini river were the locations where these occurrences took place. In addition, the majority of landslides occurred simultaneously at very shallow and quite deep soil levels. When doing previous research on landslip susceptibility mapping or hazard zonation, it was common practice to overlook the slope aspect. Solar radiation, which may play a significant role in the deterioration of rocks, has the potential to affect weathering processes, and the slope may also have an impact on these processes. According to the findings of this research, slopes that face southeast, south, or west are the most likely to have landslides. A conclusion may be drawn from this that the metropolitan areas and agricultural land that are facing this direction are at danger. Due to the fact that the Main Central Thrust (MCT) goes through the Chamoli district, it is located in a very seismically active region due of its location. The findings make it quite evident that this particular research area, and more specifically the region that is immediately around the Main Central Thrust (MCT), is extremely susceptible to landslides. On the other hand, the processes that cause landslides in the Indian Himalayan Region are rather complicated. In these systems, geologic conditions play a regulating function; nevertheless, external forces also play a role in the evolution of these systems. According to the findings of this research, the likelihood of landslides occurring in regions that experience significant

ISSN:2731-538X | E-ISSN:2731-5398

Vol. 17 No. 02 (2023)

rainfall as a result of climate change is higher. This was described in Section 2.1. As a result, landslides that are caused by rainfall pose a significant threat to human operations, in addition to posing an increased danger to both property and human life. When you need to map and analyse the susceptibility of landslides in the future, make advantage of the new and complete geology data, high-resolution datasets, and external elements that are related to spatial data such as the strength and duration of rainfall and the intensity of earthquakes. Locations that were more than one thousand metres away from the lineament, as well as those that were buried in snow or glaciers, did not suffer landslides. To add insult to injury, we still do not know how much of a role temperature, groundwater, and snowmelt play in the danger of landslides, despite the fact that these factors most likely do play a role. After taking into account the fact that the research was conducted on a regional scale (1936.06 km2), we believe that the findings were adequate.

By constructing a multi-temporal landslide inventory, it is possible to acquire a more precise mapping of landslide susceptibility as well as a better image of the immediate and long-term consequences that landslide occurrences have on ecosystems. Landslides in this research region are often caused by precipitation, flash floods, and cloudbursts, among other similar phenomena. The result of this was that we documented all of the landslides that took place between the years 2011 and 2013 as a consequence of a variety of occurrences, including cloudbursts, flash floods, and heavy rains. The landslides that occurred were produced by a number of different events, including cloudbursts, flash floods, and intense rainfall. It is possible that our landslide susceptibility map has benefits over previous work done in this landslide-prone region, which relied on a single incidence to establish vulnerability. Furthermore, according to the landslide susceptibility map that was developed by a number of researchers, the areas of the Mandakini river catchment that were located at lower to intermediate catchment levels and higher elevations were less likely to have landslides, thereby resulting in the formation of a low landslide hazard zone. Whatever the case may be, these regions were emphasised in a significant way on our landslip risk map. This is due to the fact that these regions had a significant number of landslides during the years 2011 and 2013. Furthermore, a number of landslips have been seen in hilly parts of India and the Himalayan region as a consequence of both natural and man-made sources. These landslips have occurred in combination with one another. This landslide-prone region is hard to overlook because of the ongoing human intervention in land cover caused by development projects. The Indian Himalayas are especially fragile, and this interference makes it impossible to ignore this region. Because of all of these factors, it is possible that there may be other landslides in this region. Both the Kedarnath temple, which is a significant pilgrimage destination, and the Kedarnath sanctuary, which is located in the upper Mandakini river basin, have contributed to the study area's historical and cultural significance. Therefore, our landslip susceptibility map may be of use to local governments in the areas of land use planning, the reduction of landslip risk, and the preservation of beautiful landscapes.

ISSN:2731-538X | E-ISSN:2731-5398

Vol. 17 No. 02 (2023)

CONCLUSIONS

The Himalayan region and hilly regions of India face significant issues as a result of the prevalence of landslides. For the purpose of ensuring the safety of human occupations, the development of infrastructure, and the conservation of the landscape in this area that is prone to landslides, landslide susceptibility mapping is an essential technology for locating potentially hazardous locations. The purpose of this research was to show the broad use of BHUVAN in combination with the construction of a multi-temporal landslide inventory (polygon data) in order to develop a landslide susceptibility map in the Chamoli area, which had a limited amount of data. On the basis of past research, supplementary resources, and fieldwork, fifteen different elements that have the potential to cause landslides were taken into serious consideration. As a further step, we used a quantitative strategy, which encompassed the TLS and UAV approaches, as a component of the bivariate statistical procedure. The objective was to eliminate the subjectivity that was present in weights and to identify the circumstances that contributed to the development of the BIS and APH methodologies. A prediction accuracy of 85.7% was attained by the model that used the UAV and TLS technique. This suggests that the model achieved a pretty high degree of accuracy. Due to the presence of the Kedarnath temple, which is a pilgrimage destination, as well as the animal sanctuary, the territory under investigation became crucial. This Chamoli area landslip susceptibility map, which the local authorities might utilise, could be beneficial for a number of purposes, including land use planning, landscape protection, and the reduction of landslip hazards. There is still a dearth of a sufficient landslip database and body of study in the Himalayas and other biodiverse regions. It is difficult to do more study on landslide hazard related assessment in the Indian Himalayan area because there is a shortage of resources. These resources include a thorough inventory of landslides that have occurred over the course of time, high-resolution satellite pictures that are inexpensive, and extensive records of previous landslides. As a result, we have presented a detailed analysis of the current level of landslip inventory, vulnerability mapping, and risk assessment in India. This study includes a discussion of the gaps, the current advancements, and the future directions. The Chamoli region in the Indian Himalayan Region, which is prone to landslides, serves as an example in this study, which fills in some of the gaps that were identified by earlier research.

REFERENCES

1. Larson, K. P., Godin, L., & Price, R. A. (2010). Relationships between displacement and distortion in orogens: Linking the Himalayan foreland and hinterland in central Nepal. Bulletin, 122(7-8), 1116-1134.

ISSN:2731-538X | E-ISSN:2731-5398

Vol. 17 No. 02 (2023)

2. Tobgay, T., McQuarrie, N., Long, S., Kohn, M. J., & Corrie, S. L. (2012). The age and rate of displacement along the Main Central Thrust in the western Bhutan Himalaya. Earth and Planetary Science Letters, 319, 146-158.

3. Cooper, F. J., Adams, B. A., Edwards, C. S., & Hodges, K. V. (2012). Large normal-sense displacement on the South Tibetan fault system in the eastern Himalaya. Geology, 40(11), 971-974.

4. Bhattacharya, A., & Mukherjee, K. (2017). Review on InSAR based displacement monitoring of Indian Himalayas: issues, challenges and possible advanced alternatives. Geocarto International, 32(3), 298-321.

5. Yesilnacar, E.; Topal, T. Landslide susceptibility mapping: A comparison of logistic regression and neural networks methods in a medium scale study, Hendek region (Turkey). Eng. Geol. 2005, 79, 251–266.

6. Magliulo, P.; Di, L.A.; Russo, F.; Zelano, A. Geomorphology and landslide susceptibility assessment using GIS and bivariate statistics: A case study in southern Italy. Nat Hazards 2008, 47, 411.

7. Fawcett, T. An introduction to roc analysis. Pattern Recognit. Lett. 2006, 27, 861–874.

8. Samia, J.; Temme, A.; Bregt, A.K.; Wallinga, J.; Stuiver, J.; Guzzetti, F.; Ardizzone, F.; Rossi, M. Implementing landslide path dependency in landslide susceptibility modelling. Landslides 2018, 15, 2129–2144.

9. Dai, F.C.; Lee, C.F.; Ngai, Y.Y. Landslide risk assessment and management: An overview. Eng. Geol. 2002, 64, 65–87.

10. Dahal, R.K.; Hasegawa, S.; Masuda, T.; Yamanaka, M. Roadside slope failures in Nepal during torrential rainfall and their mitigation. Disaster Mitig. Debris Flowsslope Fail. Landslides 2006, 2, 503–514.

11. Tropeano, D.; Turconi, L. Using historical documents for landslide, debris flow and stream flood prevention. Applications in northern Italy. Nat. Hazards 2004, 31, 663–679.

12. Van Beek, L.P.H.; Van Asch, T.W.J. Regional assessment of the effects of land-use change on landslide hazard by means of physically based modelling. Nat. Hazards 2004, 31, 289–304.

ISSN:2731-538X | E-ISSN:2731-5398

Vol. 17 No. 02 (2023)

13. Gorsevski, P.V.; Gessler, P.E.; Foltz, R.B.; Elliot, W.J. Spatial Prediction of Landslide Hazard Using Logistic Regression and ROC Analysis. Trans. GIS 2006, 10, 395–415.

14. Raghuvanshi, T.K.; Ibrahim, J.; Ayalew, D. Slope stability susceptibility evaluation parameter (SSEP) rating scheme—An approach for landslide hazard zonation. J. Afr. Earth Sci. 2014, 99, 595–612.

15. Kanungo, D.P.; Arora, M.K.; Sarkar, S.; Gupta, R.P. A comparative study of conventional, ANN black box, fuzzy and combined neural and fuzzy weighting procedures for landslide susceptibility zonation in Darjeeling Himalayas. Eng. Geol. 2006, 85, 347–366.

16. Fell, R.; Corominas, J.; Bonnard, C.; Cascini, L.; Leroi, E.; Savage, W.Z. Guidelines for landslide susceptibility, hazard and risk zoning for land use planning. Eng. Geol. 2008, 102, 85–98.

17. Promper, C.; Puissant, A.; Malet, J.P.; Glade, T. Analysis of land cover changes in the past and the future as contribution to landslide risk scenarios. Appl. Geogr. 2014, 53, 11–
19.

18. Batar, A.K.; Watanabe, T.; Kumar, A. Assessment of Land-Use/Land-Cover Change and Forest Fragmentation in the Garhwal Himalayan Region of India. Environments 2017, 4, 34.

19. Meusburger, K.; Alewell, C. Impacts of anthropogenic and environmental factors on the occurrence of shallow landslides in an alpine catchment (Urseren Valley, Switzerland). Nat. Hazards Earth Syst. Sci. 2008, 8, 509–520.

20. Reichenbach, P.; Busca, C.; Mondini, A.C.; Rossi, M. Land use change scenarios and landslide susceptibility zonation: The Briga Catchment Test Area (Messina, Italy). In Engineering Geology for Society and Territory; Lollino, G., Manconi, A., Clague, J., Eds.; Springer International Publishing: Berlin/Heidelberg, Germany, 2015; Volume 1, pp. 557–561.

21. Schuster, R.; Highland, L. The Third Hans Cloos Lecture. Urban landslides: Socioeconomic impacts and overview of mitigative strategies. Bull. Eng. Geol. Environ. 2007, 66, 1–27.

22. Geertsema, M.; Pojar, J.J. The influnce of landslides on biophysical diversity—A perspective from British Columbia. Geomorphology 2007, 89, 55–69.

ISSN:2731-538X | E-ISSN:2731-5398

Vol. 17 No. 02 (2023)

23. Gunther, A.; Thiel, C. Combined rock slope stability and shallow landslide susceptibility assessment of the Jasmund Cliff area (Ru¨gen Island, Germany). Nat. Hazards Earth Syst.
Sci. 2009, 9, 687–698

24. Hasegawa, S.; Dahal, R.K.; Nishimura, T.; Nonomura, A.; Yamanaka, M. DEM-based analysis of earthquake-induced shallow landslide susceptibility. Geotech. Geol. Eng. 2009, 27, 419–430.

25. Mavrouli, O.; Corominas, J.; Wartman, J. Methodology to evaluate rock slope stability under seismic conditions at Sola‘ de Santa Coloma, Andorra. Nat. Hazards Earth Syst. Sci. 2009, 9, 1763–1773. [CrossRef]

26. Van Westen, C.J.; Rengers, N.; Soeters, R. Use of geomorphological information in indirect landslide susceptibility assessment. Nat. Hazards 2003, 30, 399–419

27. Pradhan, B.; Youssef, A.M. Manifestation of remote sensing data and GIS on landslide hazard analysis using spatial-based statistical models. Arab. J. Geosci. 2009, 3, 319–326.

28. Oh, H.J.; Lee, S.; Hong, M. Landslide Susceptibility Assessment Using Frequency Ratio Technique with Iterative Random Sampling. J. Sens. 2017, 2017, 1–22.

29. Ewen, J.; Parkin, G.; O’Connell, P.E. SHETRAN: Distributed river basin flow and transport modeling system. J. Hydrol. Eng. 2000, 5, 250–258.

30. Baum, R.L.; Savage, W.Z.; Godt, J.W. TRIGRS—A Fortran program for transient rainfall infiltration and grid-based regional slope-stability analysis. US Geol. Surv. Open-File Rep. 2002, 424, 38.